Available online at www.sciencedirect.com
SCIENCE DIRECT®
International Journal of Heat and Mass Transfer 48 (2005) 2140–2149
International Journal of HEAT and MASS TRANSFER
www.elsevier.com/locate/ijhmt

A fixed-grid approach for diffusion- and reaction-controlled wet chemical etching

P. Rath [a], J.C. Chai [a,*], H. Zheng [b], Y.C. Lam [a], V.M. Murukeshan [a], H. Zhu [a]

[a] School of Mechanical and Production Engineering, Nanyang Technological University, Singapore 639798, Singapore
[b] Singapore Institute of Manufacturing Technology, Singapore 638075, Singapore

Received 30 July 2004; received in revised form 31 December 2004
Available online 17 March 2005

Abstract

A new mathematical model for wet chemical etching process is presented. The proposed method is a fixed-grid approach based on the total concentration of etchant. It is analogous to the enthalpy method used in the modeling of melting/solidification problems. The total concentration is the sum of the unreacted etchant concentration and the reacted etchant concentration. The reacted etchant concentration is used to capture the etchfront. The governing equation based on the total concentration is formulated. This governing equation is shown to be equivalent to the conventional governing equation. It also contains the interface condition. A procedure to update the reacted concentration is presented. Numerical results for one-dimensional diffusion-controlled and reaction-controlled etching are presented.

1. Introduction

Wet chemical etching (WCE) is an important lithographic process for the fabrication of electronic devices. It is a process of removing a small layer of material from the substrate surface by chemical reaction with a reagent material called etchant to give a specific pattern on the substrate surface. WCE process is widely applicable in manufacturing shadow mask for color-television tubes [1], IC devices in microelectronics industries [2], MEMS devices such as hinges [3] and pressure sensors [4] etc.

WCE has been modeled using asymptotic solution [5], moving grid (MG) approach [6–11] and level-set method [12–14]. One-dimensional [10] and two-dimensional [5–9,11] diffusion-controlled [5–9] and reaction-controlled [6,8–11] etching were examined. The effects of natural and forced convection were studied by Shin and Economou [8,9].

Kuiken [5] presented an asymptotic solution for WCE. The substrate is partly protected by a mask making it a two-dimensional problem. The solution is valid for diffusion-controlled etching using dilute etchant.

The most widely used approach for WCE is the MG method. In the MG method, the etchant domain is discretized and the etchant concentration is solved using appropriate boundary conditions and a specified initial condition. The etchfront velocities are then calculated and the computational domain enlarged to account for the depletion of the substrate. The process is repeated until the desired etch depth has been achieved or when the specified etching time has been reached. As the computational domain expands with time, the computation mesh is regenerated at every time step. Due to the

* Corresponding author. Tel.: +65 6790 4270; fax: +65 6792 4062.
E-mail address: mckchai@ntu.edu.sg (J.C. Chai).

0017-9310/$ - see front matter © 2005 Elsevier Ltd. All rights reserved.
doi:10.1016/j.ijheatmasstransfer.2004.12.033

Nomenclature

a	coefficient of the discretization equation
C	unreacted etchant concentration
C_R	reacted etchant concentration
$C_{R,max}$	maximum possible value of the reacted concentration
C_T	total concentration
D	diffusion coefficient
k	rate constant of reaction
M_{Sub}	molecular weight of the substrate
m	stoichiometric reaction parameter
t	time
v	velocity of the interface
x	coordinate direction

List of abbreviations

DG	Deal–Grove model
FG	fixed grid method
MG	moving grid method
ECV	etching control volume
FVM	finite volume method
WCE	wet chemical etching

Greek symbols

α	underrelaxation factor
Δt	time step
ρ_{Sub}	density of the substrate
β	non-dimensional etching parameter

Subscripts

0	initial
P	control volume P
Sub	the substrate
Et	the etchant

Superscripts

m	iteration number
0	previous time step

movement of the mesh, the mesh velocities must be accounted for. As a result of the mesh velocities, a diffusion problem becomes a convection-diffusion problem and a convection term must be included in the governing equation [6,11]. Further, an unstructured mesh or a body-fitted grid system is needed to model multidimensional WCE [6,8,9,11].

Vuik and Cuvelier [6] model two-dimensional WCE using a MG approach. The governing equation was discretized using the finite-difference method. Both diffusion-controlled and reaction-controlled etchings were modeled. Mesh velocities due to the expanding computational domain were included in the model. Kuiken et al. [7] presented an exact solution for diffusion-controlled etching in a one-dimensional geometry. In the same paper a two-dimensional numerical approach for diffusion-controlled etching based on MG method is also presented. The finite-difference method was used to discretize the governing equation and the effect of grid velocities is neglected. Shin and Economou [8] studied the effect of flowing etchant on the shape evolution of two-dimensional etched cavities using the MG approach. The finite-element method was employed to solve for the fluid velocity profiles and for the etchant concentration distributions in cavities of arbitrary shapes. In this model, the extra convective term due to grid velocities was neglected. It has been found that with fluid flow in the cavity, the time-averaged etch rate increased four times and the time-averaged etch anisotropy increased by 40% as compared to pure diffusion under condition studied. The etch anisotropy is a measure of mask undercut during etching. For perfect anisotropic etching, there is no mask undercut. Shin and Economou [9] compared the effects of forced and natural convection on the shape evolution of deep etching cavities. Forced convection was found to be very ineffective for etching deep cavities. The etching rate decreased sharply with time as the cavity became deeper during etching. At the same time, the etching rate distribution along the active surface (the substrate surface in contact with etching fluid where reaction is taking place) became nearly uniform, degrading etch anisotropy. In contrast, natural convection was effective for rinsing the dissolution products (products of reaction) out of the cavity. Li et al. [10] used MG approach to predict the etch rate of phosphosilicate-glass (PSG) in hydrofluoric acid (HF) for radial geometry. The etchant solution is assumed to be stationary and mesh velocities were not included in the model. The reaction assumed to be mixed order i.e. a combination of first and second order reaction kinetics. Kaneko et al. [11] used a MG approach to model reaction-controlled WCE of an aluminium substrate using the finite-element method. Two-dimensional etching is considered and a first order reaction kinetic is assumed. The extra convective term due to grid velocities was also taken into account in this model. Adalsteinsson and Sethian [12,13] simulated two- and three-dimensional deposition, etching, and lithography in integrated circuit fabrication using a level-set model. La Magna et al. [14] used a level-set method to simulate two-dimensional reaction-controlled etching process.

In this article, a fixed-grid (FG) method [15] for WCE is presented in detail. A total concentration which is the sum of unreacted etchant concentration and reacted etchant concentration is defined in the proposed FG method. In this formulation, the reacted concentration of etchant is a measure of the etch depth. Since the grid size is fixed, there is no grid velocity. Hence a diffusion problem always remains a diffusion problem. Cartesian grid can be used to capture the complicated etchfront in multidimensional etching problems. The proposed method is analogous to the enthalpy method used in the modeling of melting/solidification process [16–32].

The remainder of this article is divided into six sections. In the next section, a one-dimensional WCE problem, the governing equation, the interface condition and the boundary conditions are described. Various ingredients of the proposed FG approach are discussed in the following section. In this section, a new concentration is defined. The governing equation based on the newly defined total concentration which contains the interface condition, is formulated. A procedure to update the reacted concentration is also presented. The overall solution procedure is then summarized. A brief description of the numerical method used in this article follows. A discussion of the results obtained using the proposed FG method is given. Some concluding remarks are given to conclude the article.

2. Problem description

The schematic and coordinate system used for the one-dimensional geometry considered in this article is shown in Fig. 1. The initial etchant concentration at $t = 0$ is C_0. At $t > 0$, the reaction between the etchant and the substrate at the etchant–substrate interface results in the reduction of the concentration of etchant adjacent to the etchant–substrate interface and the depletion of the substrate. The origin of the coordinate system is set to the etchant–substrate interface at $t = 0$. With this definition, the coordinates of the region occupied by the substrate at $t = 0$ is negative. The governing equation, the interface condition and the boundary conditions are presented next.

2.1. Governing equation

For a quiescent etchant solution, the etchant concentration within the etchant domain is governed by the mass diffusion equation given by

$$\frac{\partial C}{\partial t} = \frac{\partial}{\partial x}\left(D\frac{\partial C}{\partial x}\right) \tag{1}$$

where C, D, t and x are the concentration of the etchant, the diffusion coefficient of the etchant, the time and the distance respectively. Strictly speaking, there is another etchant concentration equation within the substrate domain. Since the etchant concentration is zero within the substrate at all time, this equation is not solved.

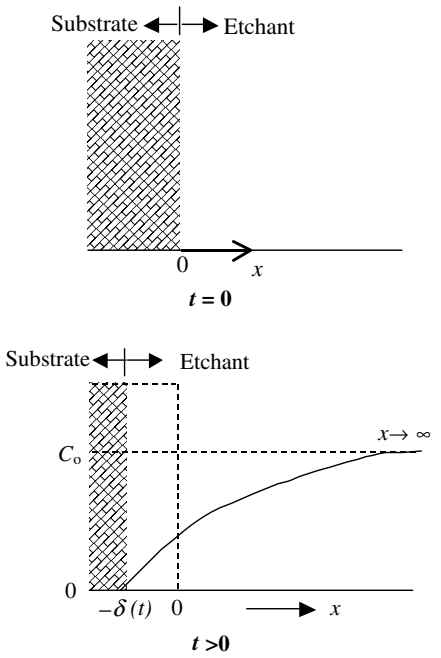

Fig. 1. Schematic of a one-dimensional etching problem and coordinate system.

2.2. Interface condition

For the situation shown in Fig. 1, the interface condition at the etchant–substrate interface is given by

$$D\frac{\partial C}{\partial x} = \frac{m\rho_{\mathrm{Sub}}}{M_{\mathrm{Sub}}}\frac{\mathrm{d}\delta}{\mathrm{d}t} = \frac{m\rho_{\mathrm{Sub}}}{M_{\mathrm{Sub}}}v \tag{2}$$

where m, ρ_{Sub}, M_{Sub}, δ and v are the stoichiometric reaction parameter, the density of the substrate, the molecular weight of the substrate, the etch depth and the velocity of the etchfront respectively.

2.3. Boundary conditions

There are two boundary conditions associated with the governing equation (Eq. (1)): one at the etchant–substrate interface and another at the "free" boundary (i.e. opposite to the etchant–substrate interface). The mass diffusion flux at the interface is related to the reaction rate. For a first order reaction in the coordinate system as shown in Fig. 1, the mass diffusion flux is given as

$$D\frac{\partial C}{\partial x} = kC \quad \text{at } x = -\delta(t) \tag{3}$$

where k is the rate constant of the reaction. The boundary condition at the "free" boundary is given as

$$C = C_0 \quad \text{at } x \to \infty \tag{4}$$

3. Mathematical formulation

A FG method is proposed in this article. Various ingredients of the proposed FG method are presented in this section.

3.1. Total concentration

In the proposed FG method, a new variable called the *total* concentration is defined as

$$C_T \equiv C + C_R \tag{5}$$

where C_T, C and C_R are the total concentration, the (unreacted) etchant concentration and the reacted (etchant) concentration respectively. Physically, C_R is the etchant concentration consumed in the reaction process. As such it is constant except at the etchant–substrate interface. This is used to capture the etchfront implicitly. The value of C_R changes from 0 to its maximum possible value of $C_{R,max}$ in a control volume where etching is taking place. The maximum possible value of the reacted concentration ($C_{R,max}$) is the amount of etchant required per unit volume of substrate to dissolve the substrate during reaction. The exact expression for $C_{R,max}$ will be derived later.

3.2. Governing equation

A governing equation in-terms of the total concentration is derived in this section. Consider a one-dimensional control volume of thickness dx and cross-sectional area A_c. In the absence of convection, mass balance in the control volume dx, can be written as

$$J_x - J_{x+dx} = \frac{d}{dt}(C_T A_c\, dx) \tag{6}$$

In Eq. (6), the three terms are the rate of moles of species into the control volume dx, the rate of moles of species leaving the control volume dx and the rate of change of total moles of species inside the control volume dx respectively. Eq. (6) can be rewritten as

$$\frac{d}{dt}(C_T A_c\, dx) = J_x - \left[J_x + \frac{\partial}{\partial x}(J_x)\, dx\right] = -\frac{\partial}{\partial x}(J_x)\, dx \tag{7}$$

Using the Fick's law, Eq. (7) can be written as

$$\frac{dC_T}{dt} = \frac{\partial}{\partial x}\left(D\frac{\partial C}{\partial x}\right) \tag{8}$$

Eq. (8) is the governing equation based on the *total* concentration. This equation is valid in both the etchant and the substrate regions. The interface condition given by Eq. (2) is contained in Eq. (8) implicitly. This is shown next.

3.3. Interface condition

Using Eq. (8), the integral form of the governing equation based on the total concentration for a one-dimensional control volume spanning $x_l \leqslant x \leqslant x_u$ can be written as

$$\frac{d}{dt}\int_{x_l}^{x_u} C_T\, dx = \int_{x_l}^{x_u} \frac{\partial}{\partial x}\left(D\frac{\partial C}{\partial x}\right) dx = \left(D\frac{\partial C}{\partial x}\right)_{x_u} - \left(D\frac{\partial C}{\partial x}\right)_{x_l} \tag{9}$$

Consider an elementary control volume of length L ($L = L_e + L_s$, which contains the interface) as shown in Fig. 2 at two time intervals. Between t and $t + \Delta t$, an Δx-thick layer of substrate has been etched away. Locations of the interface at time t and at time $t + \Delta t$ are shown in Fig. 2. The total concentrations at t and $t + \Delta t$ are

$$\int_{-L_s}^{L_e} C_T^t\, dx = \int_{-L_s}^{-\Delta x} (C_T^t)_{Sub}\, dx + \int_{-\Delta x}^{0} (C_T^t)_{Sub}\, dx + \int_0^{L_e} (C_T^t)_{Et}\, dx \tag{10}$$

and

$$\int_{-L_s}^{L_e} C_T^{t+\Delta t}\, dx = \int_{-L_s}^{-\Delta x} (C_T^{t+\Delta t})_{Sub}\, dx + \int_{-\Delta x}^{0} (C_T^{t+\Delta t})_{Et}\, dx + \int_0^{L_e} (C_T^{t+\Delta t})_{Et}\, dx \tag{11}$$

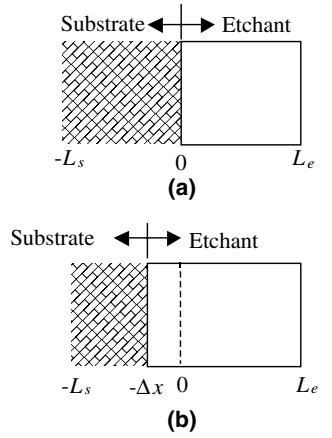

Fig. 2. Etchant–substrate interface locations at two time steps: (a) time t and (b) time $t + \Delta t$.

where the subscripts Et and Sub represent the total concentrations in the etchant and the substrate regions respectively. Subtracting Eq. (10) from Eq. (11), gives

$$\int_{-L_s}^{L_e}\left(C_T^{t+\Delta t}-C_T^{t}\right)\mathrm{d}x=\int_{-L_s}^{-\Delta x}\left(C_T^{t+\Delta t}-C_T^{t}\right)_{\mathrm{Sub}}\mathrm{d}x+\int_{-\Delta x}^{0}\left[\left(C_T^{t+\Delta t}\right)_{\mathrm{Et}}-\left(C_T^{t}\right)_{\mathrm{Sub}}\right]\mathrm{d}x+\int_{0}^{L_e}\left(C_T^{t+\Delta t}-C_T^{t}\right)_{\mathrm{Et}}\mathrm{d}x \tag{12}$$

Dividing both sides by Δt, and taking limits as $\Delta t \to 0$ gives

$$\frac{\mathrm{d}}{\mathrm{d}t}\int_{-L_s}^{L_e}C_T\,\mathrm{d}x=\frac{\mathrm{d}}{\mathrm{d}t}\int_{-L_s}^{-\Delta x}\left(C_T\right)_{\mathrm{Sub}}\mathrm{d}x+\lim_{\Delta t\to 0}\int_{-\Delta x}^{0}\frac{\left[\left(C_T^{t+\Delta t}\right)_{\mathrm{Et}}-\left(C_T^{t}\right)_{\mathrm{Sub}}\right]}{\Delta t}\mathrm{d}x+\frac{\mathrm{d}}{\mathrm{d}t}\int_{0}^{L_e}\left(C_T\right)_{\mathrm{Et}}\mathrm{d}x \tag{13}$$

Using Eq. (9), Eq. (13) can be written as

$$\frac{\mathrm{d}}{\mathrm{d}t}\int_{-L_s}^{L_e}C_T\,\mathrm{d}x=\left(D\frac{\partial C}{\partial x}\right)_{\mathrm{Sub},-\Delta x}-\left(D\frac{\partial C}{\partial x}\right)_{-L_s}+\lim_{\Delta t\to 0}\int_{-\Delta x}^{0}\frac{\left[\left(C_T^{t+\Delta t}\right)_{\mathrm{Et}}-\left(C_T^{t}\right)_{\mathrm{Sub}}\right]}{\Delta t}\mathrm{d}x+\left(D\frac{\partial C}{\partial x}\right)_{L_e}-\left(D\frac{\partial C}{\partial x}\right)_{\mathrm{Et},0} \tag{14}$$

Eq. (14) can be rearranged as

$$\frac{\mathrm{d}}{\mathrm{d}t}\int_{-L_s}^{L_e}C_T\,\mathrm{d}x-\left[\left(D\frac{\partial C}{\partial x}\right)_{L_e}-\left(D\frac{\partial C}{\partial x}\right)_{-L_s}\right]=\lim_{\Delta t\to 0}\int_{-\Delta x}^{0}\frac{\left[\left(C_T^{t+\Delta t}\right)_{\mathrm{Et}}-\left(C_T^{t}\right)_{\mathrm{Sub}}\right]}{\Delta t}\mathrm{d}x+\left(D\frac{\partial C}{\partial x}\right)_{\mathrm{Sub},-\Delta x}-\left(D\frac{\partial C}{\partial x}\right)_{\mathrm{Et},0} \tag{15}$$

Using Eq. (9), Eq. (15) reduces to

$$\left(D\frac{\partial C}{\partial x}\right)_{\mathrm{Et},0}-\left(D\frac{\partial C}{\partial x}\right)_{\mathrm{Sub},-\Delta x}=\lim_{\Delta t\to 0}\int_{-\Delta x}^{0}\frac{\left[\left(C_T^{t+\Delta t}\right)_{\mathrm{Et}}-\left(C_T^{t}\right)_{\mathrm{Sub}}\right]}{\Delta t}\mathrm{d}x \tag{16}$$

In the substrate, the unreacted etchant concentration is zero. As a result, the second term of Eq. (16) vanishes and Eq. (16) becomes

$$\left(D\frac{\partial C}{\partial x}\right)_{\mathrm{Et},0}=\lim_{\Delta t\to 0}\int_{-\Delta x}^{0}\frac{\left[\left(C_T^{t+\Delta t}\right)_{\mathrm{Et}}-\left(C_T^{t}\right)_{\mathrm{Sub}}\right]}{\Delta t}\mathrm{d}x \tag{17}$$

As $\Delta t \to 0$, the ratio $\mathrm{d}x/\Delta t$ approaches v, where v is the local normal velocity of the interfacial surface element towards the substrate region. Attention is now focused on the remaining terms. At time t, the interface is occupied by the substrate. As the interface is occupied by the substrate, the reacted concentration is zero. The unreacted concentration at the interface is finite. As a result, the total concentration is

$$\left(C_T^{t}\right)_{\mathrm{Sub}}=C^{t}+C_R^{t}=C^{t} \tag{18}$$

At time $t+\Delta t$, the total concentration is

$$\left(C_T^{t+\Delta t}\right)_{\mathrm{Et}}=C^{t+\Delta t}+C_R^{t+\Delta t} \tag{19}$$

From Fig. 2(b), a layer of substrate has been etched away and the vacated space is now filled with the etchant. As $\Delta t \to 0$, the unreacted concentration $C^{t+\Delta t} \to C^{t}$ and the reacted concentration $C_R^{t+\Delta t} \to C_{R,\max}$. Hence Eq. (19) reduces to

$$\left(C_T^{t+\Delta t}\right)_{\mathrm{Et}}=C^{t}+C_{R,\max} \tag{20}$$

Using Eqs. (18) and (20), Eq. (17) becomes

$$D\frac{\partial C}{\partial x}=C_{R,\max}v \tag{21}$$

The exact expression for $C_{R,\max}$ is now derived. In a unit volume, there are $\rho_{\mathrm{Sub}}/M_{\mathrm{Sub}}$ moles of substrate. The reaction between the etchant and the substrate can be represented as

$$S+mE\rightarrow qP \tag{22}$$

where S, E and P are the substrate, the etchant and the product respectively. From Eq. (22) it is seen that the amount of etchant needed to dissolve a unit volume of substrate is $m\rho_{\mathrm{Sub}}/M_{\mathrm{Sub}}$. As $C_{R,\max}$ is the amount of etchant required per unit volume of substrate to dissolve the substrate during reaction, it can therefore be written as

$$C_{R,\max}=\frac{m\rho_{\mathrm{Sub}}}{M_{\mathrm{Sub}}} \tag{23}$$

Using Eq. (23), Eq. (21) becomes

$$D\frac{\partial C}{\partial x}=\frac{m\rho_{\mathrm{Sub}}}{M_{\mathrm{Sub}}}v \tag{24}$$

which is the interface condition given in Eq. (2).

3.4. Procedure to update C_R

A procedure to calculate the reacted etchant concentration C_R is presented in this section. The governing equation (Eq. (8)) is rewritten using Eq. (5) as

$$\frac{\partial C}{\partial t}=\frac{\partial}{\partial x}\left(D\frac{\partial C}{\partial x}\right)-\frac{\partial C_R}{\partial t} \tag{25}$$

As the reacted concentration is constant away from the etchant–substrate interface, Eq. (25) reduces to the original governing equation (Eq. (1)) except at the etchant–substrate interface. At the etchant–substrate interface, the reacted etchant concentration is a measure of the

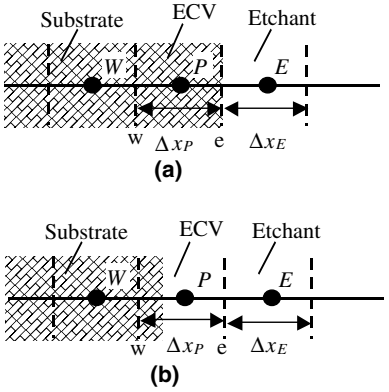

Fig. 3. A control volume (P) undergoing etching: (a) the ECV when etching starts and (b) the ECV during etching.

amount of substrate being etched. In the proposed FG method, a control volume (Fig. 3) where etching is taking place is identified and called the etching control volume (ECV). In this ECV, C_R changes from 0 to its maximum possible value $C_{R,max}$. A procedure to update C_R in the ECV is described in this section. The finite volume discretized equation (using implicit scheme) of Eq. (25) for a control volume P (control volume undergoing etching i.e. ECV) as shown in Fig. 3 is given as

$$a_P C_P^m = \sum a_{nb} C_{nb}^m + a_P^0 C_P^0 - (C_{R,P}^m - C_{R,P}^0)\frac{\Delta x_P}{\Delta t} \tag{26}$$

where m, 0, P, nb, a, Δx and Δt are the mth iteration of the current time step, the previous time step, the control volume P, the neighboring control volumes, the coefficients of the discretization equation, the volume of a control volume, and the time step respectively. Eq. (26) is valid for all control volumes. However, as C_R is constant in the etchant and substrate, the last term on the right side of Eq. (26) is zero except in the ECV. At the $(m+1)$th iteration, Eq. (26) can be written as

$$a_P C_P^{m+1} = \sum a_{nb} C_{nb}^{m+1} + a_P^0 C_P^0 - (C_{R,P}^{m+1} - C_{R,P}^0)\frac{\Delta x_P}{\Delta t} \tag{27}$$

Subtracting Eq. (27) from Eq. (26) and rearranging, gives

$$C_{R,P}^{m+1} = C_{R,P}^m + \frac{\Delta t}{\Delta x_P}\left[a_P(C_P^m - C_P^{m+1}) + \sum a_{nb}(C_{nb}^{m+1} - C_{nb}^m)\right] \tag{28}$$

When the solution converges, the last term of Eq. (28) will be zero. However, during the initial iteration process, it is most likely a non-zero term. Realizing that it is zero upon convergence, this term can be ignored from the calculation and Eq. (28) becomes

$$C_{R,P}^{m+1} = C_{R,P}^m + \alpha a_P \frac{\Delta t}{\Delta x_P}(C_P^m - C_P^{m+1}) \tag{29}$$

where α is the under-relaxation parameter. Eq. (29) is used in updating the reacted concentration in the ECV. In Eq. (29), C_P^{m+1} is approximated as

$$C_P^{m+1} = \frac{1}{2}(C_e^m + C_w^m) \tag{30}$$

where C_e^m and C_w^m are the east and the west interface concentrations of ECV and these are approximated using Eq. (3) as

$$C_e^m = \frac{C_E^m}{1 + \frac{k_e}{D_e}\frac{\Delta x_E}{2}} \tag{31a}$$

$$C_w^m = \frac{C_P^m}{1 + \frac{k_w}{D_w}\frac{\Delta x_P}{2}} \tag{31b}$$

where Δx_P and Δx_E are widths of the control volume ECV and an adjacent control volume to the east of ECV as shown in Fig. 3.

3.5. Initialization of the etchant concentration in the ECV

When etching starts in an ECV, the initial unreacted etchant concentration of the ECV is approximated using the boundary condition at the interface as given in Eq. (3). Consider an ECV as shown in Fig. 3, which has two interfaces—e and w respectively. From Eq. (3), the nodal concentration when etching *starts* in the ECV is given as

$$D_P\frac{C_e^m - C_w^m}{\Delta x_P} = k_P C_P^m \tag{32}$$

Using Eq. (31a) and (31b), C_P^m can be written as

$$C_P^m = \frac{C_E^m}{\left(1 + \frac{k_e \Delta x_E}{2D_e}\right)\left[\frac{k_P \Delta x_P}{D_P} + \frac{1}{1 + \frac{k_w \Delta x_P}{2D_w}}\right]} \tag{33}$$

4. Overall solution procedure

The overall solution procedure for the proposed FG method based on the total concentration can be summarized as follows:

1. Specify the etchant and the substrate domains. Ensure that the etchant–substrate interface lies on the interface between two control volumes.
2. Set the initial etchant concentration as C_0 in the etchant domain and 0 in the substrate domain.
3. Initially set C_R to 0 in the substrate domain and $C_{R,max}$ in the etchant domain respectively.
4. Advance the time step to $t + \Delta t$.
5. Identify the etching control volumes. These are the substrate control volumes with adjacent etchant control volumes.

6. Set the etchant concentration of the previous time step and initialize the etchant concentration of the current time step in the ECV using Eq. (33).
7. Solve Eq. (25) for the concentration.
8. Update the reacted concentration in the ECV using Eq. (29).
9. Check for convergence.
   [a] If solution has not converged, check the calculated reacted concentration.
   - If $C_R < C_{R,max}$, repeat (7) to (8).
   - If $C_R \geqslant C_{R,max}$, then set $C_R = C_{R,max}$ and repeat (5) to (8).

   [b] If solution has converged, then check if the number of time steps has been reached. If yes, stop. If not, repeat (4) to (8).

5. Numerical method

In this article, the finite-volume method (FVM) of Patankar [33] is used to solve the concentration equation. Since a detailed discussion of the FVM is available in Patankar [33], only a very brief description of the major features of the FVM used is given here.

In the FVM, the domain is divided into a number of control volumes such that there is one control volume surrounding each grid point. The grid point is located in the center of a control volume. The governing equation is integrated over each control volume to derive an algebraic equation containing the grid point values of the dependent variable. The discretization equation then expresses the conservation principle for a finite control volume just as the partial differential equation expresses it for an infinitesimal control volume. The resulting solution implies that the integral conservation of mass is exactly satisfied for any control volume and of course, for the whole domain. The resulting algebraic equations are solved using a line-by-line tri-diagonal matrix algorithm. In the present study, a solution is deemed converged when the maximum change in the concentration and the maximum change in the reacted concentration between two successive iterations are less than 10^{-11}.

6. Results and discussion

The one-dimensional problem shown in Fig. 1 is modeled using the proposed FG method. The initial etchant and substrate thicknesses are set to 0.03 cm and 51 μm respectively. The density and molecular weight of the substrate are taken to be 2.1 g/cm^3 and 60 respectively. The stoichiometric reaction parameter is 6. The diffusion coefficient of etchant is 10^{-5} cm^2/s. The concentration at the "free" boundary (i.e. opposite to the etchant–substrate interface) is kept at the initial concentration C_0. A dimensionless variable β is used to present the results. This variable is defined as

$$\beta \equiv \frac{m\rho_{Sub}/M_{Sub}}{C_0} \tag{34}$$

From Eq. (34), β is inversely proportional to the initial etchant concentration C_0.

6.1. Diffusion-controlled etching

In diffusion-controlled etching the reaction rate at the interface is infinitely fast compared to diffusion of etchant to the interface. Therefore, for a given diffusion coefficient of etchant, if $k \gg D$, then the etching process can be assumed diffusion-controlled. Fig. 4 shows the grid independent study for four spatial grid sizes namely, 12 μm, 6 μm, 3 μm and 1.5 μm. The time step is kept at 0.001 s and further reduction in the time step does not alter the solution. Fig. 4a shows the etch depth versus time plot with $\beta = 2$. It can be seen that all four spatial grids capture the etchfront accurately. Fig. 4b shows the concentration distributions at $t = 4$ s.

Fig. 5 shows the comparisons of the etch depth and concentration distributions for four β values. The

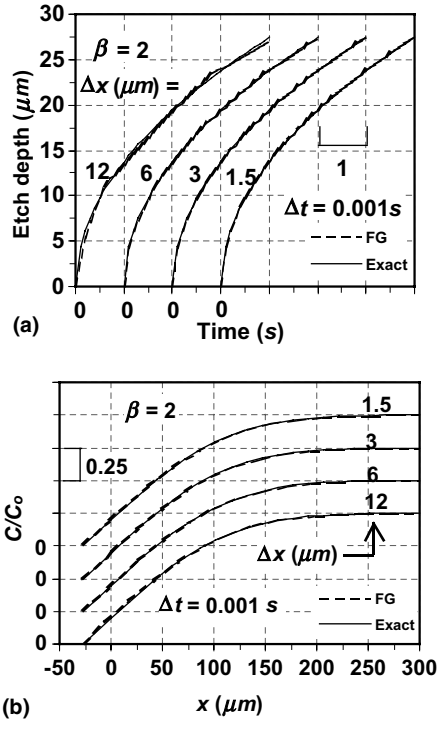

Fig. 4. Grid independent test for $\beta = 2$ and $D = 10^{-5}$ cm^2/s in diffusion-controlled etching ($k \gg D$): (a) variation of etch depths for 4 s of etching and (b) concentration distributions at $t = 4$ s.

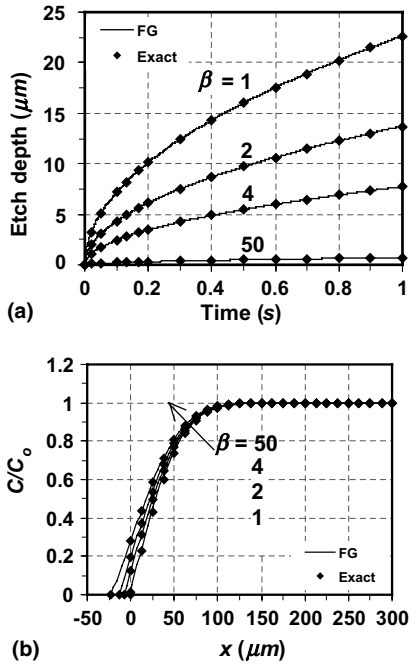

Fig. 5. Comparisons of FG and exact solution [7] for $D = 10^{-5}$ cm^2/s and four β values in diffusion-controlled etching ($k \gg D$): (a) variation of etch depths for 1 s of etching and (b) concentration distributions at $t = 1$ s.

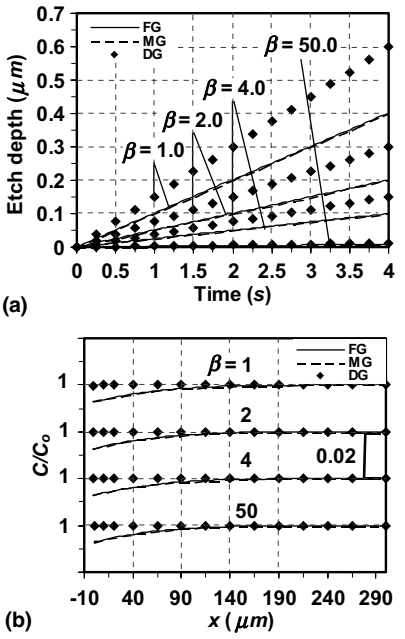

Fig. 6. Comparisons of FG, MG and DG models for four β values in reaction-controlled etching with $k = 10^{-5}$ cm/s and $D = 10^{-5}$ cm^2/s: (a) variation of etch depths for 4 s of etching and (b) concentration distributions at $t = 4$ s.

control volume size and the time step size used in FG method are 1.5 μm and 0.001 s respectively. The etch depth and concentration distributions obtained using the proposed approach are compared with the exact solutions [7]. Kuiken et al. derived the exact solution for concentration distribution and etch depth variation for etching in semi-infinite etchant medium. Fig. 5a shows the etch depths variations for 1 s of etching and Fig. 5b shows the concentration distributions at $t = 1$ s for four β values. It is also seen that as the value of β increases, the etch depth decreases. This is because β is inversely proportional to the initial etchant concentration C_0 for a given etchant–substrate combination.

6.2. Reaction-controlled etching

In the reaction-controlled etching the reaction rate is finite. For the test problem considered here, the rate constant of reaction is taken as, $k = 10^{-5}$ cm^2/s. Fig. 6a shows the etch depths over 4 s for four β values. An approximate analytical solution called the Deal–Grove (DG) model [34,35] is also shown for completeness. The FG solutions agree well with the MG results. The DG model however overpredicts the etch depths. This is especially true at smaller β values. Fig. 6b shows the concentration profiles at $t = 4$ s for four β values. Again, the FG and MG solutions agree well. The DG model assumes negligible change in the concentration of etchant in the etchant medium (see Fig. 6b). As a result, the DG model overpredicts the etch depth as shown in Fig. 6a.

Effects of the rate of reaction on etch depth and concentration distributions are shown in Fig. 7 for $\beta = 1$. A range of k values is selected to study the effect of the rate of reaction. It is seen from Fig. 7a that as k increases, the etch depth increases at a given time. The increase in k means reaction rate increases at the interface. Hence etching of substrate is increased which leads to larger etch depth at a given time. Under a limiting case when the reaction rate is infinitely fast i.e. $k \gg D$, the etching process is said to be diffusion-controlled. From Fig. 7a it is seen that when $k \geqslant 0.1$ cm/s, the etching can be considered diffusion-controlled as further increase in k does not alter the etch depth and the concentration distributions. For a given diffusion coefficient of etchant, the highest etch depth in a given time is obtained when the etching is diffusion-controlled.

From Fig. 7b, it is seen that the etchant concentration at the etchant–substrate interface remains at the initial concentration when $k = 10^{-5}$ cm/s. At this value of k, the reaction is slow and any etchant consumed in the etching process is replenished via diffusion. The etchant concentration at the interface decreases as the value of k increases. It is zero when $k \geqslant 0.1$ cm/s. As mentioned, at this value of k, the etching is diffusion-controlled

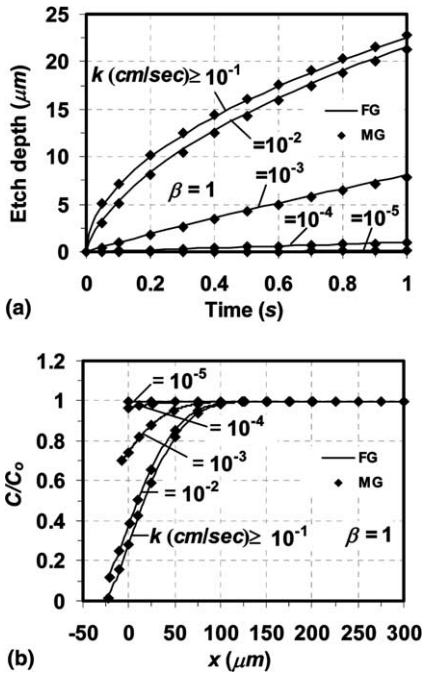

Fig. 7. Comparisons of FG and MG methods for a range of k values with $D = 10^{-5}$ cm^2/s and $\beta = 1$: (a) variation of etch depths for 1 s of etching and (b) concentration distributions at $t = 1$ s.

and from Eq. (3) the etchant concentration at the interface is zero.

7. Concluding remarks

A new mathematical model based on the fixed-grid approach has been presented. The proposed method is analogous to the enthalpy method used in the modeling of melting/solidification processes. A detailed formulation based on the total concentration of the etchant is presented. In the proposed approach the governing equation includes the interface condition. With this proposed method the etchfront position need not be coupled explicitly. The method has been applied to one-dimensional diffusion-controlled and reaction-controlled etchings. For demonstration purposes, the finite-volume method is used to discretize the governing equation. The results show that the etch depth and the etchant concentration are predicted accurately using the proposed method. Since the grid size is fixed and the computation domain is the whole etchant and substrate domain, the proposed method can be easily extended to model multidimensional etching problems. In multidimensional cases, there are more than one etching control volumes where reaction can occur simultaneously. In such cases etching control volumes can be identified using the same procedure as discussed in this article.

References

[1] K.H. Hoffman, J. Sprekels, Free boundary problems: Theory and applications, Longman Sci. Tech. 1 (1990) 89.
[2] M.J. Madou, Fundamentals of Microfabrication, 2nd ed., CRC Press, New York, 2002.
[3] K.S.J. Pister, M.W. Judy, S.R. Burgett, R.S. Fearing, Microfabricated hinges, Sensors Actuators A 33 (1992) 249–256.
[4] C.H. Mastrangelo, X. Zhang, W.C. Tang, Surface micromachined capacitive differential pressure sensor with lithographically-defined silicon diaphragm, The Eighth International Conference on Solid-State Sensors and Actuators, Eurosensor IX, Stockholm, 25–29 June 1995, pp. 612–615.
[5] H.K. Kuiken, Etching: A two-dimensional mathematical approach, Proc. Royal Soc. London A 392 (1984) 199–225.
[6] C. Vuik, C. Cuvelier, Numerical solution of an etching problem, J. Comput. Phys. 59 (1985) 247–263.
[7] H.K. Kuiken, J.J. Kelly, P.H.L. Notten, Etching profiles at resist edges, J. Electrochem. Soc. 133 (1986) 1217–1226.
[8] C.B. Shin, D.J. Economou, Effect of transport and reaction on the shape evolution of cavities during wet chemical etching, J. Electrochem. Soc. 136 (1989) 1997–2004.
[9] C.B. Shin, D.J. Economou, Forced and natural convection effects on the shape evolution of cavities during wet chemical etching, J. Electrochem. Soc. 138 (1991) 527–538.
[10] W.J. Li, J.C. Shih, J.D. Mai, C-M. Ho, J. Liu, Y-C. Tai, Numerical simulation for the sacrificial release of MEMS square diaphragms, 1st International Conference on MSMSSA, San Jose, USA, April, 1998.
[11] K. Kaneko, T. Noda, M. Sakata, T. Uchiyama, Observation and numerical simulation for wet chemical etching process of semiconductor, in: Proceedings of Fourth ASME-JSME Joint Fluids Engineering Conference, Honolulu, USA, 6–10 July 2003.
[12] D. Adalsteinsson, J.A. Sethian, A level set approach to a unified model for etching, deposition, and lithography I: Algorithms and two-dimensional simulations, J. Comput. Phys. 120 (1995) 128–144.
[13] D. Adalsteinsson, J.A. Sethian, A level set approach to a unified model for etching, deposition, and lithography II: Three-dimensional simulations, J. Computat. Phys. 122 (1995) 348–366.
[14] A. La Magna, G. D'Arrigo, G. Garozzo, C. Spinella, Computational analysis of etched profile evolution for the derivation of 2D dopant density maps in silicon, Mater. Sci. Eng. B 102 (1–3) (2003) 43–48.
[15] Y.C. Lam, J.C. Chai, P. Rath, H. Zheng, V.M. Murukeshan, A fixed grid method for chemical etching, Int. Commun. Heat Mass Transfer 31 (8) (2004) 1123–1131.
[16] N. Shamsundar, E.M. Sparrow, Analysis of multidimensional conduction phase change via the enthalpy method, J. Heat Transfer 97 (1975) 333–340.
[17] N. Shamsundar, E. Rooz, Numerical methods for moving boundary problems, in: W.J. Minkowycz, E.M. Sparrow, G.E. Schneider, R.H. Pletcher (Eds.), Handbook of Numerical Heat Transfer, 1st ed., Wiley, New York, 1988, pp. 747–786.

[18] A.D. Brent, V.R. Voller, K.J. Reid, Enthalpy-porosity technique for modeling convection-diffusion phase change: Application to the melting of a pure metal, Numer. Heat Transfer 13 (1988) 297–318.
[19] V.R. Voller, An overview of numerical methods for solving phase change problems, in: W.J. Minkowycz, E.M. Sparrow (Eds.), Advances in Numerical Heat Transfer, vol. 1, Taylor and Francis, 1997, pp. 344–359.
[20] C.K. Chun, S.O. Park, A fixed-grid finite-difference method for phase-change problems, Numer. Heat Transfer Part B 38 (1) (2000) 59–73.
[21] J. Jaidi, P. Dutta, Modeling of transport phenomena in a gas metal arc welding process, Numer. Heat Transfer Part A 40 (5) (2001) 543–562.
[22] D.M. Christopher, Comparison of interface-following techniques for numerical analysis of phase-change problems, Numer. Heat Transfer Part B 39 (2) (2001) 189–206.
[23] I. Ahmed, T.L. Bergman, An engineering model for solid-liquid phase change within sprayed ceramic coatings of nonuniform thickness, Numer. Heat Transfer Part A 41 (2) (2002) 113–129.
[24] M. Giangi, F. Stella, E. Leonardi, G. de Vahl Davis, A numerical study of solidification in the presence of a free surface under microgravity conditions, Numer. Heat Transfer Part A 41 (6–7) (2002) 579–595.
[25] C. Benjapiyaporn, G. de Vahl Davis, E. Leonardi, S.S. Leong, V. Timchenko, H.C. de Groh III, A numerical study of G-Jitter during directional solidification, Numer. Heat Transfer Part A 41 (6–7) (2002) 597–610.
[26] S. Sarkar, P. Mohan Raj, S. Chakraborty, P. Dutta, Three-dimensional computational modeling of momentum, heat, and mass transfer in a laser surface alloying process, Numer. Heat Transfer Part A 42 (3) (2002) 307–326.
[27] J. Kaenton, G. de Vahl Davis, E. Leonardi, S.S. Leong, A numerical study of anisotropy and convection during solidification, Numer. Heat Transfer Part B 41 (3–4) (2002) 309–323.
[28] M. Pasandideh-Fard, S. Chandra, J. Mostaghimi, A three-dimensional model of droplet impact and solidification, Int. J. Heat Mass Transfer 45 (11) (2002) 2229–2242.
[29] M. Bhattacharya, T. Basak, K.G. Ayappa, A fixed-grid finite element based enthalpy formulation for generalized phase change problems: Role of superficial mushy region, Int. J. Heat Mass Transfer 45 (24) (2002) 4881–4898.
[30] S. Chakraborty, N. Chakraborty, P. Kumar, P. Dutta, Studies on turbulent momentum, heat and species transport during binary alloy solidification in a top-cooled rectangular cavity, Int. J. Heat Mass Transfer 46 (7) (2003) 1115–1137.
[31] T. Basak, Analysis of resonances during microwave thawing of slabs, Int. J. Heat Mass Transfer 46 (22) (2003) 4279–4301.
[32] J. Kaenton, E. Semma, V. Timchenko, M. El Ganaoui, E. Leonardi, G. de Vahl Davis, Effects of anisotropy and solid/liquid thermal conductivity ratio on flow instabilities during inverted Bridgman growth, Int. J. Heat Mass Transfer 47 (14–16) (2004) 3403–3413.
[33] S.V. Patankar, Numerical Heat Transfer and Fluid Flow, 1st ed., Hemisphere, New York, 1980.
[34] D.J. Monk, D.S. Soane, R.T. Howe, Sacrificial layer SiO_2 wet etching for micromachining applications, International Conference on Solid-State Sensors and Actuators, San Francisco, CA (Transducers '91), 1991, pp. 647–650.
[35] J. Liu, Y-C. Tai, J. Lee, K-C. Pong, Y. Zohar, C-M. Ho, In situ monitoring and universal modeling of sacrificial PSG etching using hydrofluoric acid, IEEE 0-7803-0957-2/93 (1993).